Progress In Electromagnetics Research, PIER 96, 309–328, 2009

CHARACTERIZATION OF THE VALIDITY REGION OF THE EXTENDED T-MATRIX METHOD FOR SCATTERING FROM DIELECTRIC CYLINDERS WITH FINITE LENGTH

W. Z. Yan and Y. Du

The Department of Information Science and Electronics Engineering
Zhejiang University
Hangzhou 310027, China

Z. Y. Li and E. X. Chen

Institute of Forest Resources Information Techniques
Chinese Academy of Forestry
Beijing 100091, China

J. C. Shi

Institute for Computational Earth System Sciences
University of California
Santa Barbara, CA 93106, USA

Abstract—The T-matrix approach is effective in analyzing electromagnetic scattering from finite scatterers. Yet for scatterers with extreme geometry, this approach may fail. One example is its inability to analyze scattering from dielectric cylinders with large aspect ratios. To deal with such difficulty, recently we proposed a method based on an extension of the T-matrix approach, where a long cylinder is hypothetically divided into a cluster of identical sub-cylinders, for each the T matrix can be numerically stably calculated. Special care was paid to fulfill the boundary conditions at the hypothetic surface of any two neighboring sub-cylinders. The resultant coupled equations are different from that of multi-scatterer theory. The model results were in good agreement with experiment data available in the literature. However, the validity region of the proposed method was not fully characterized. Now we have developed and validated a method of moment (MoM) code, and are in a position to carry on the task of

Corresponding author: Y. Du (zjuydu03@zju.edu.cn).

characterizing the validity region. The proposed method is found to be applicable to dielectric cylinders of arbitrary length as long as the T matrix is attainable for the elementary sub-cylinder. The conditions for the T matrix to be numerically stably calculated in terms of the equivalent volumetric radius and relative dielectric constant are also empirically obtained.

1. INTRODUCTION

The electromagnetic scattering by canonical physical objects is important in many applications [1–8]. For the case of dielectric cylinder with finite length, an exact analytical solution is still elusive, and several approximation approaches have been proposed in the literature. One popular approach is the generalized Rayleigh-Gans (GRG) approximation [9, 10], where the induced current in the cylinder is approximated by that of infinite length. This method is valid for a needle shaped scatterer with radius much smaller than the wavelength. It should be noted that solutions of such approximate methods in general fail to satisfy the reciprocity theorem.

On the other hand, a semi-analytical method called the T-matrix approach [11] is based on the extended boundary condition method (EBCM), with the T matrix being used to relate the exciting field and scattered field, where the exciting field is assumed to be inside the inscribing sphere and the scattered field outside the circumscribing sphere, respectively. The T-matrix approach is gaining popularity due to its rigor and powerfulness and has been applied to scattering from objects of various shapes, such as spheroids, finite cylinders, Chebyshev particles, cubes, clusters of spheres, and so on [12–17].

However, in treating scattering from dielectric cylinder of finite length, if any of the parameters including length, equivalent volumetric radius, and relative dielectric constant is adequately large, then the T-matrix approach may suffer from slow convergence or even fail to converge [18]. With a focus on ensuring convergence for dielectric cylinders with large aspect ratio (the ratio of length to diameter of a cylinder), recently we have proposed a new iterative technique with extension to the T-matrix approach [19], where a long cylinder is hypothetically divided into a cluster of identical sub-cylinders, for each the T matrix can be numerically stably calculated. Special care was paid to fulfill the boundary conditions at the hypothetic surface of any two neighboring sub-cylinders. The resultant coupled equations are different from that of multi-scatterer theory. The model results were in good agreement with experiment data available in the literature.

However, the validity region of the proposed method was not fully characterized. To this end, we have developed and verified a MoM code, which is based on the combined-field integral equation (CFIE) with Galerkins procedure [20], and are in a position to carry on the task of characterizing the validity region. The proposed method is found to be applicable to dielectric cylinders of arbitrary length as long as the T matrix is attainable for the elementary sub-cylinder. The conditions for the T matrix to be numerically stably calculated in terms of the equivalent volumetric radius and relative dielectric constant are also empirically obtained.

2. T-MATRIX APPROACH

In T-matrix approach, the incident, scattered, and internal fields are expressed in terms of the spherical harmonics, respectively

$$\begin{aligned}
\mathbf{E}^{inc}\left(\bar{r}'\right) &= \sum_{n,m}\left\{a_{mn}^{inc(M)} Rg\bar{M}_{mn}\left(\bar{r}'\right) + a_{mn}^{inc(N)} Rg\bar{N}_{mn}\left(\bar{r}'\right)\right\} \\
\mathbf{E}^{sca}\left(\bar{r}'\right) &= \sum_{n,m}\left\{a_{mn}^{sca(M)} \bar{M}_{mn}\left(\bar{r}'\right) + a_{mn}^{sca(N)} \bar{N}_{mn}\left(\bar{r}'\right)\right\} \\
\mathbf{E}^{int}\left(\bar{r}'\right) &= \sum_{n,m}\left\{a_{mn}^{int(M)} Rg\bar{M}_{mn}\left(\bar{r}'\right) + a_{mn}^{int(N)} Rg\bar{N}_{mn}\left(\bar{r}'\right)\right\}
\end{aligned} \tag{1}$$

where $Rg\bar{M}_{mn}$, $Rg\bar{N}_{mn}$, $\bar{M}_{mn}$ and $\bar{N}_{mn}$ are the vector spherical waves respectively as defined in [25]. Owing to the linearity of Maxwell's equations and boundary conditions, the linear relation between the scattered field coefficients $\bar{a}^{sca}$ and the incident field coefficients $\bar{a}^{inc}$ can be related by a system transfer operator called T-matrix as follows [11]:

$$\bar{a}^{sca} = \bar{\bar{T}}\,\bar{a}^{inc}. \tag{2}$$

Note that matrix T in (2) contains the full information about the wave scattering and absorption properties of a object. A very attractive feature of the T-matrix approach is that, unlike many other methods of analyzing scattering where the entire calculation needs to be repeated for each new incident field, the T matrix only needs to be calculated once because it is independent of any specific incident field. Moreover, utilizing geometrical symmetries of scatterers can drastically reduce CPU-time requirements.

In analyzing scattering from dielectric cylinders of finite length, the applicability of the T-matrix approach depends on the frequency of the incidence wave, and describing parameters of the cylinder including length, equivalent volumetric radius, and relative dielectric

constant. When none of the describing parameters is large, the T-matrix method is applicable [18]. One example is shown in Fig. 1 where the theoretical results of T-matrix method for both vertical and horizontal polarization bistatic scattering cross section are in agreement of that of MoM. In this example, the diameter D of cylinder is 2 cm, the length L is 6 cm and the relative dielectric constant ϵ_r is $4 + i$. The frequency of the incidence wave is 5 GHz, and the elevation angle of incident wave is 105° and the azimuthal angle is 90°. The cylinder is located at the origin and its symmetric axis is along z axis. In our treatment of MoM, all the surfaces of cylinders are approximated by planar triangular patches where the edge length is set to $\lambda/8$ and the Rao-Wilton-Glisson (RWG) function [21] is chosen as both basis and test functions. The developed code has been tested extensively against FEKO, a commercial software product for the simulation of electromagnetic fields, and excellent agreement is always obtained. One illustration is shown in Fig. 2, where the simulation parameters are as above except $L = 11$ cm. Both vertical- and horizontal-polarized bistatic scattering cross sections almost completely overlap for the developed MoM code and FEKO.

On the other hand, if any of the parameters becomes large, the T-matrix approach may suffer from convergence problem or converges to incorrect values [18]. For example, if we keep the same configuration as that of the example in Fig. 1 except that the length is enlarged to 11 cm, then we would be alarmed to observe that the predictive power of the T-matrix method has drastically degraded (see Fig. 3).

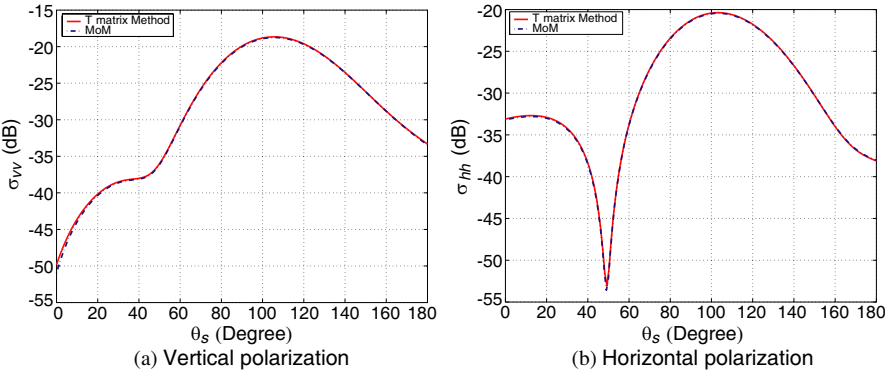

Figure 1. The bistatic scattering cross section of a circular cylinder under conventional T-matrix method and MoM where the length is 6 cm and diameter is 2 cm.

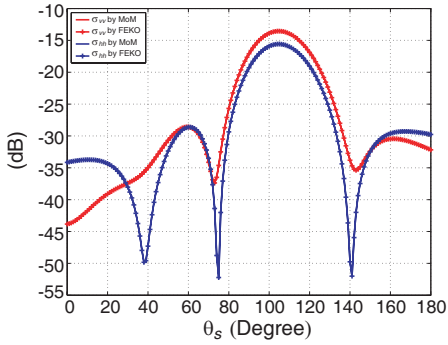

Figure 2. The bistatic scattering cross section of a circular cylinder under the developed MoM code and FEKO where the length is 11 cm and diameter is 2 cm.

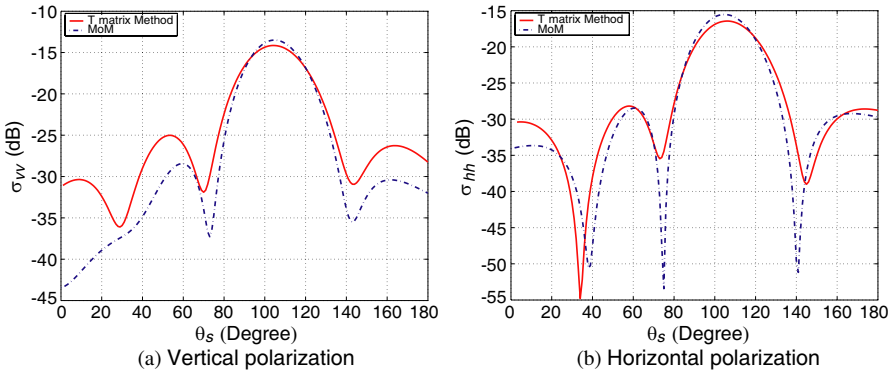

(a) Vertical polarization (b) Horizontal polarization

Figure 3. The bistatic scattering cross section of a circular cylinder under conventional T-matrix method and MoM where the length is 11 cm and diameter is 2 cm.

3. BRIEF DESCRIPTION OF THE PROPOSED ITERATIVE METHOD

It is understood that in the conventional form of the T-matrix formalism, its applicability to scattering from dielectric cylinders of finite length is limited. Any attempt to extend the range of applicability of the T-matrix approach starts from an analysis of the characteristics of the issues at hand. In earth observation using microwave remote sensing means, when tree or crop constituents such as trunks, stems or branches are typically modelled as dielectric cylinders of finite length (e.g., [22, 23]), their diameters or relative

dielectric constants are in general within the reach of T-matrix method at L, C or X band. The major concern is the large aspect ratio. To this end we have recently developed a new iterative technique with extension to the T-matrix approach [19] which we shall briefly describe as follows.

In this method, an elongated cylinder is first divided into a cluster of N identical sub-cylinder by using $N-1$ hypothetic surfaces, for each the T matrix can be calculated stably in the numerical sense. Then special care is paid to both rigorously fulfill the boundary conditions at the hypothetical division interfaces and cast the coupling among sub-cylinder into a rigorous formulism. For illustration purpose, the case of two sub-cylinder division is considered here (Fig. 4). Since the EBCM involves surface integrals and since cylinder division generates hypothetical interfaces, these surfaces need to be denoted carefully before we proceed. Each sub-cylinder will contain a primary surface and an interface. We shall start number ordering from the lowest sub-cylinder (see Fig. 4). The center of sub-cylinder j is r_j. The primary surface of sub-cylinder $j(j = 1, 2)$, S_{jp}, includes its surface without the division interface. The common interface is denoted by S_{12}.

$$\begin{bmatrix} a_{mn}^{(M)(j)v} \\ a_{mn}^{(N)(j)v} \end{bmatrix} = -ik(-1)^m \int_{S_v} dS \left\{ i\omega\mu\hat{n}_j \times \mathbf{H}_{\mathrm{j}}(\mathbf{r}) \cdot \begin{bmatrix} \bar{M}_{-mn}(\overline{rr}_j) \\ \bar{N}_{-mn}(\overline{rr}_j) \end{bmatrix} + k\hat{n}_j \times \mathbf{E}_{\mathrm{j}}(\mathbf{r}) \cdot \begin{bmatrix} \bar{N}_{-mn}(\overline{rr}_j) \\ \bar{M}_{-mn}(\overline{rr}_j) \end{bmatrix} \right\} \tag{3}$$

$$\begin{bmatrix} a_{mn}^{s(M)(j)v} \\ a_{mn}^{s(N)(j)v} \end{bmatrix} = ik(-1)^m \int_{S_v} dS \left\{ i\omega\mu\hat{n}_j \times \mathbf{H}_{\mathrm{j}}(\mathbf{r}) \cdot \begin{bmatrix} Rg\bar{M}_{-mn}(\overline{rr}_j) \\ Rg\bar{N}_{-mn}(\overline{rr}_j) \end{bmatrix} + k\hat{n}_j \times \mathbf{E}_{\mathrm{j}}(\mathbf{r}) \cdot \begin{bmatrix} Rg\bar{N}_{-mn}(\overline{rr}_j) \\ Rg\bar{M}_{-mn}(\overline{rr}_j) \end{bmatrix} \right\} \tag{4}$$

Because the boundary conditions at the division interface of each sub-cylinder are pointwise while the EBCM is in an integral form and should be carefully incorporated into the EBCM formalism, thus for such concern, we introduce some intermediate variables that have specific meanings, where the fields are expanded in terms of vector spherical waves with different origins and the boundary conditions are incorporated. Such variables are expressed in (3) and (4), where the superscript $v(v = p, d)$ denotes the primary part (p) or common interface (d) of the jth sub-cylinder, and corresponding S_v denotes S_{jp} or S_{12}, respectively. s denotes the scattered field. In the above, $\hat{n}_j$ is the outward pointing unit normal vectors on the surface S_j of sub-cylinder j. These intermediate variables are not arbitrary quantities

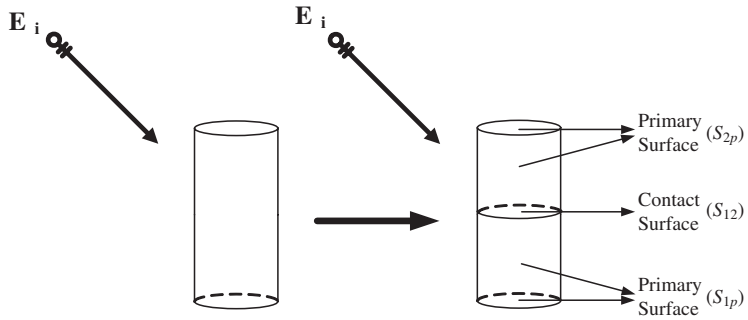

Figure 4. Division of a cylinder into two identical sub-cylinder.

but have specific physical meanings. They represent the expansion coefficients of the exciting fields and scattered fields due to the primary surfaces and the interface of these sub-cylinder, respectively. Therefore, utilizing T matrix, the expanded coefficients $\bar{a}_{mn}$ and $\bar{a}^s_{mn}$ for each part can be related.

Since the quantities $\bar{a}^{(1)u}_{mn}$ and $\bar{a}^{s(2)d}_{mn}$ are expressed in terms of the tangential fields on the interface, it is natural to relate them in some way. Yet since each involves vector spherical waves with different origins, a transformation of origin must first be performed using the translational addition theorem which is a powerful analytic tool to solve theoretically for the scattering properties of multiple scatterers. For the case of vector spherical wave functions, the vector addition theorems have the form [24]

$$\begin{bmatrix} Rg\bar{M}_{mn}(\bar{r}_j) \\ Rg\bar{N}_{mn}(\bar{r}_j) \end{bmatrix} = \sum_{\mu,\nu} \left\{ \begin{bmatrix} RgA^{mn}_{\mu\nu}(\bar{r}_{ji}) \\ RgB^{mn}_{\mu\nu}(\bar{r}_{ji}) \end{bmatrix} Rg\bar{M}_{\mu\nu}(\bar{r}_i) + \begin{bmatrix} RgB^{mn}_{\mu\nu}(\bar{r}_{ji}) \\ RgA^{mn}_{\mu\nu}(\bar{r}_{ji}) \end{bmatrix} Rg\bar{N}_{\mu\nu}(\bar{r}_i) \right\} \tag{5}$$

and

$$\begin{bmatrix} \bar{M}_{mn}(\bar{r}_j) \\ \bar{N}_{mn}(\bar{r}_j) \end{bmatrix} = \sum_{\mu,\nu} \left\{ \begin{bmatrix} A^{mn}_{\mu\nu}(\bar{r}_{ji}) \\ B^{mn}_{\mu\nu}(\bar{r}_{ji}) \end{bmatrix} Rg\bar{M}_{\mu\nu}(\bar{r}_i) + \begin{bmatrix} B^{mn}_{\mu\nu}(\bar{r}_{ji}) \\ A^{mn}_{\mu\nu}(\bar{r}_{ji}) \end{bmatrix} Rg\bar{N}_{\mu\nu}(\bar{r}_i) \right\} \tag{6}$$

for the condition $\bar{r}_i < \bar{r}_{ji}$, where the vector spherical waves with and without the prefix Rg stand for regular and outgoing waves, respectively. The formulation and computation of coefficients $A^{mn}_{\mu\nu}$ and $B^{mn}_{\mu\nu}$ also can be found in [24]. Fortunately, for the transformation in

this case we have the convenience of reducing the double summation over m and ν to single summation over ν because the translation is along the z axis. By shifting the origin from r_1 to r_2 and making use of the intermediate variables of sub-cylinder 2, the term $\bar{a}_{mn}^{(1)d}$ can thus be expressed as

$$\begin{bmatrix} a_{mn}^{(M)(1)d} \\ a_{mn}^{(N)(1)d} \end{bmatrix} = \sum_{\nu} \left\{ A_{-mn}^{-m\nu}(\overline{r_1 r}_2) \begin{bmatrix} a_{m\nu}^{s(M)(2)d} \\ a_{m\nu}^{s(N)(2)d} \end{bmatrix} + B_{-mn}^{-m\nu}(\overline{r_1 r}_2) \begin{bmatrix} a_{m\nu}^{s(N)(2)d} \\ a_{m\nu}^{s(M)(2)d} \end{bmatrix} \right\}. \tag{7}$$

Here,we also specifically make use of the boundary conditions $\hat{n}_1 \times \mathbf{H}_1 = -\hat{n}_2 \times \mathbf{H}_2$ and $\hat{n}_1 \times \mathbf{E}_1 = -\hat{n}_2 \times \mathbf{E}_2$.

Note that for a single scatterer, the incident field is equal to the exciting field. In our case, the virtual partition shall not change this property. Now if we let the global origin coincidence with r_1, by applying transformation of origin on the vector spherical waves and making use of the intermediate variables we have

$$\begin{bmatrix} a_{mn}^{(M)} \\ a_{mn}^{(N)} \end{bmatrix} = \begin{bmatrix} a_{mn}^{(M)(1)p} \\ a_{mn}^{(N)(1)p} \end{bmatrix} - \sum_{\nu} \left\{ A_{-m\nu}^{-mn}(\overline{r_1 r}_2) \begin{bmatrix} a_{m\nu}^{s(M)(2)p} \\ a_{m\nu}^{s(N)(2)p} \end{bmatrix} + B_{-m\nu}^{-mn}(\overline{r_1 r}_2) \begin{bmatrix} a_{m\nu}^{s(N)(2)p} \\ a_{m\nu}^{s(M)(2)p} \end{bmatrix} \right\}. \tag{8}$$

Combining the above two equations, yields

$$\begin{bmatrix} a_{mn}^{(M)} \\ a_{mn}^{(N)} \end{bmatrix} = \begin{bmatrix} a_{mn}^{(M)(1)} \\ a_{mn}^{(N)(1)} \end{bmatrix} - \sum_{\nu} \left\{ A_{-m\nu}^{-mn}(\overline{r_1 r}_2) \begin{bmatrix} a_{m\nu}^{s(M)(2)} \\ a_{m\nu}^{s(N)(2)} \end{bmatrix} + B_{-m\nu}^{-mn}(\overline{r_1 r}_2) \begin{bmatrix} a_{m\nu}^{s(N)(2)} \\ a_{m\nu}^{s(M)(2)} \end{bmatrix} \right\}. \tag{9}$$

One notes that (9) is different from that of multi-scatterer theory (MST) [25]. As a matter of fact, the MST is not valid here because its requirement of mutually exclusive circumscribing spheres of the sub-cylinders is not fulfilled.

Similarly, we can also establish the following system of equations by focusing on the upper part of cylinder as follows

$$\begin{bmatrix} a_{mn}^{(M)\prime} \\ a_{mn}^{(N)\prime} \end{bmatrix} = \begin{bmatrix} a_{mn}^{(M)(2)} \\ a_{mn}^{(N)(2)} \end{bmatrix} - \sum_{\nu} A_{-m\nu}^{-mn}(\overline{r_2 r}_1) \begin{bmatrix} a_{m\nu}^{s(M)(1)} \\ a_{m\nu}^{s(N)(1)} \end{bmatrix} - \sum_{\nu} B_{-m\nu}^{-mn}(\overline{r_2 r}_1) \begin{bmatrix} a_{m\nu}^{s(N)(1)} \\ a_{m\nu}^{s(M)(1)} \end{bmatrix}, \tag{10}$$

where the multipole coefficients of the incident plane wave $a_{mn}^{(M)'}$ and $a_{mn}^{(N)'}$ differ from $a_{mn}^{(M)}$ and $a_{mn}^{(N)}$ by a factor $e^{ikhcos\theta_i}$. Here h is the height of each sub-cylinder. Therefore, we can use iterative method to obtain the solution of these coupled, linear, simultaneous equations. The iteration procedure is summarized as follows: Starting with the initial solutions $a_{mn}^{s(M),2} = a_{mn}^{s(N),2} = 0$. From (9) and by using T matrix we obtain the new values of the scattering coefficients $\bar{a}_{mn}^{s,1}$ in (10). In a similar manner, we next use the new values to obtain the scattering coefficients $\bar{a}_{mn}^{s,2}$ in (9). The procedure is repeated until all the coefficients converge.

The scattered field can be treated similarly. Therefore, the total scattered expansion coefficients of whole cylinder in the primary coordinate system are

$$\begin{bmatrix} a_{mn}^{s(M)} \\ a_{mn}^{s(N)} \end{bmatrix} = \begin{bmatrix} a_{mn}^{s(M)(1)} \\ a_{mn}^{s(N)(1)} \end{bmatrix} + \sum_{\nu} RgA_{-m\nu}^{-mn}(\overline{r_1 r}_2) \begin{bmatrix} a_{m\nu}^{s(M)(2)} \\ a_{m\nu}^{s(N)(2)} \end{bmatrix} + \sum_{\nu} RgB_{-m\nu}^{-mn}(\overline{r_1 r}_2) \begin{bmatrix} a_{m\nu}^{s(N)(2)} \\ a_{m\nu}^{s(M)(2)} \end{bmatrix}. \quad (11)$$

In far-field region, for linear polarization the scattering cross section is defined as

$$\sigma_{pq} = 4\pi \left| F_{pq}(\hat{k}_s, \hat{k}_i) \right|^2, \quad (12)$$

where $\hat{p}$ and $\hat{q}$ are unit polarizations for the incident and scattered wave, respectively. The expression of amplitude scattering matrix $F_{pq}(\hat{k}_s, \hat{k}_i)$ is given by

$$F_{qp}(\hat{k}_s, \hat{k}_i) = \sum_{m,n} \left\{ \hat{q} \cdot a_{mn}^{s(M)total} \bar{M}_{mn}(kr, \theta, \phi) + \hat{q} \cdot a_{mn}^{s(N)total} \bar{N}_{mn}(kr, \theta, \phi) \right\} \cdot \hat{p} \quad (13)$$

where the expressions of far-field solutions for the outgoing vector spherical waves can be found in [25]. It should be noted that due to conventional EBCM has been successfully applied to particles of various shapes, the new method can also be used for finite dielectric cylinders with arbitrary cross section as long as the T matrix of each sub-cylinder can be accurately obtained.

4. CONVERGENCE CHECK AGAINST ARBITRARY ASPECT RATIO

From the numerical examples as shown in Fig. 1 and Fig. 3 we observe that applicability of the conventional T-matrix method highly depends on the aspect ratio. Its predictive results go from excellent to erroneous when the aspect ratio goes from 3 to 5.5. It is interesting to characterize the range of the aspect ratio within which the proposed iterative technique is valid.

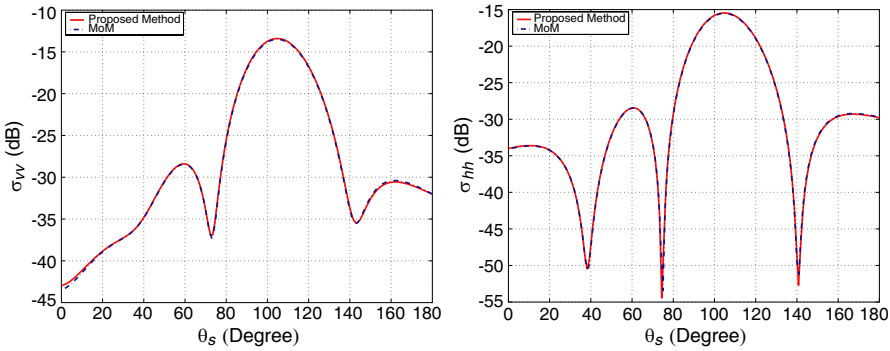

(a) Vertical polarization (b) Horizontal polarization

Figure 5. The bistatic scattering cross section of a circular cylinder under our proposed method and MoM where the length is 11 cm and diameter is 2 cm.

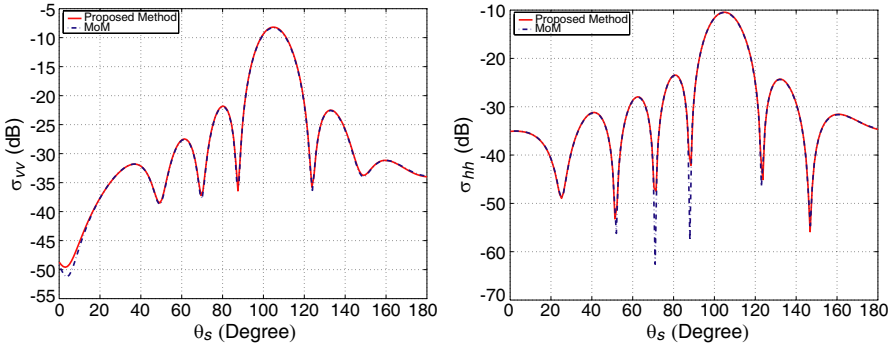

(a) Vertical polarization (b) Horizontal polarization

Figure 6. The bistatic scattering cross section of a circular cylinder under our proposed method and MoM where the length is 20 cm and diameter is 2 cm.

It should be noted that in the implementation of our proposed approach, since it involves both T matrix and translational addition theorem, and since it is well known that there are truncation errors and/or other types of errors associated with these two aspects, it is expected that any version of implementation will bear the impact of these errors to varying degree, depending on the nature of the problem at hand and the specifics of the implementation. As pointed out in [19], the truncation operations in applying addition theorem and in applying T-matrix approach are convoluted. When the number of sub-cylinders is quiet large, the iterative procedure may become an ill-conditioned one, for which caution needs to be taken. We use a method similar to the successive over-relaxation method (SOR), which takes the form of a weighted average between the previous iterate and the computed new iterate successively for each component. An extrapolation factor w $(0 \leq w \leq 1)$ is used to speed up the convergency procedure [26].

We apply the proposed method to the example of Fig. 3, where the aspect ratio ρ is 5.5. The results are shown in Fig. 5 and clearly demonstrate that, contrary to Fig. 5, both the vertically- and horizontally-polarized bistatic scattering cross sections obtained by our method are in excellent agreements with that of MoM.

We further increase the aspect ratio ρ to 10 and 20, and the results are shown in Fig. 6 and Fig. 7, respectively. Again good agreements with MoM are obtained. Continuing with other values of the aspect ratio ρ uniformly leads to the similar convergence behavior. The convergence check at different aspect ratios is tabulated in Table 1,

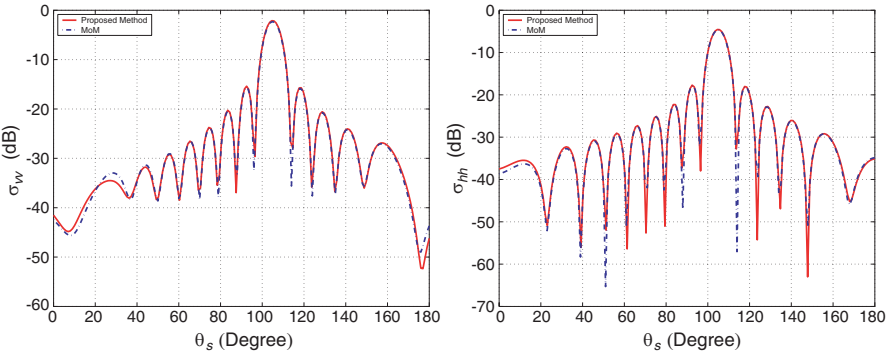

(a) Vertical polarization (b) Horizontal polarization

Figure 7. The bistatic scattering cross section of a cylinder under our proposed method and MoM where length is 40 cm and diameter is 2 cm.

where one clearly observes that for the wide range of aspect ratio (from 1 to 60), which is believed to cover the major cases of dielectric cylinders used to model constituents of plants and vegetation in nature, the proposed method always converges. It should be noted that as illustrated above, when the aspect ratio ρ goes too large (for example $\rho > 50$), the impact of truncation errors in applying the translational addition theorems and T-matrix approach becomes evident, and in addition, the condition number of the system matrix becomes larger. Yet in face of these unfavorable combinations, it is surprising to observe that agreement between the theoretical results and MoM is good except for a very small range of scattered angles.

Table 1. Convergence behaviors for cylinders with different aspect ratios where the diameter is 2 cm.

ρ	Convergence check
1	YES
3	YES
5.5	YES
10	YES
20	YES
30	YES
40	YES
50	YES
60	YES

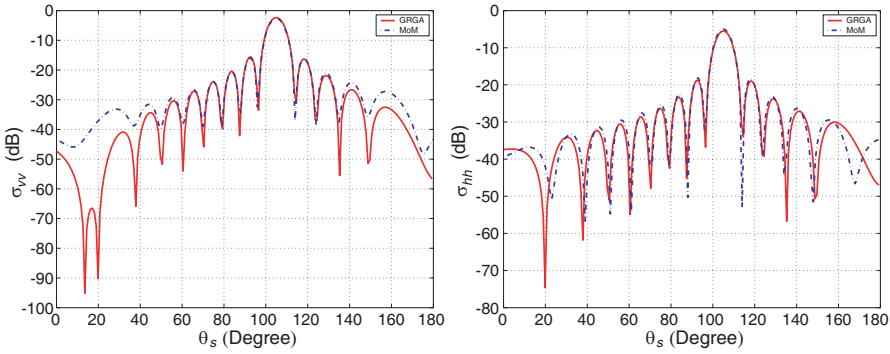

(a) Vertical polarization (b) Horizontal polarization

Figure 8. The bistatic scattering cross section of a circular cylinder under ICA and MoM where the length is 40 cm and diameter is 2 cm.

On the other hand, as a comparison, the bistatic scattering cross sections predicted by the infinite cylinder approximation (ICA) for $\rho = 20$, a case approximately satisfying the condition that the length is much larger than the diameter, are compared with MoM results (Fig. 8). ICA is obviously capable of capturing the general trend, yet appreciable discrepancy is evident, in particular at the vertical polarization. Its contrast with Fig. 7 demonstrates the fidelity of the proposed method. It should also be mentioned that aside from very high aspect ratio, ICA requires the radius of the cylinder be much smaller than wavelength, which is a condition not required in the proposed method.

5. CONVERGENCE CHECK AGAINST EQUIVALENT VOLUMETRIC RADIUS AND RELATIVE DIELECTRIC CONSTANT

In the previous section, we have demonstrated that the proposed iterative method has the appealing feature of being suitable for analyzing scattering from dielectric cylinder of large aspect ratio. Its convergence behavior against the equivalent volumetric radius (r_v) and relative dielectric constant (ϵ_r), however, is in principle determined by its sub-cylinder, which in turn speaks of the behavior of the conventional T-matrix approach.

For T-matrix computations, theoretically the multipole expansions are of infinite length and the T matrix is of infinite size. However, in practical calculations, the summation over m and n has to be truncated, thus a special procedure should be used to check the convergence of the resulting solution over the size of T matrix N_{max}. For axially symmetric scatterers, the T matrix can be decomposed into separate submatrices corresponding to different azimuthal modes m which are independently calculated. Therefore, for a desired absolute accuracy Δ of computing the expansion coefficients, the following simple convergence criterion can be used to determine $N_{\max}$, the size of T matrix [27]

$$\max\left[\left|\frac{c_1(N_{\max})-c_1(N_{\max}-1)}{c_1(N_{\max})}\right|, \left|\frac{c_2(N_{\max})-c_2(N_{\max}-1)}{c_2(N_{\max})}\right|\right] \leq \Delta, \quad (14)$$

where

$$c_1(N_{\max}) = -\frac{2\pi}{k^2} Re \sum_{n=1}^{N_{\max}} (2n+1)(T^{11}_{0n0n} + T^{22}_{0n0n}) \quad (15)$$

$$c_2(N_{\max}) = \frac{2\pi}{k^2} \sum_{n=1}^{N_{\max}} (2n+1) \left[\left|T^{11}_{0n0n}\right|^2 + \left|T^{22}_{0n0n}\right|^2\right] \quad (16)$$

It is expected that $N_{\max}$ depends on the geometry and permittivity of the cylinder. The form of dependence is clearly depicted in Fig. 9. In Fig. 9(a), $N_{\max}$ monotonically increases with the aspect ratio r_v. In Fig. 9(b), $N_{\max}$ also show a monotonic increase with the real part of dielectric constant, $Re(\epsilon_r)$. The imaginary part of dielectric constant is chosen according to Table 4, for reasons that will be clear shortly. The dependence of $N_{\max}$ on r_v and permittivity stems from the dependence of T-matrix entries on the same parameters. For instance, Fig. 10 demonstrates how the T-matrix entry T_{0101} varies with r_v, while Fig. 11 shows how T_{0101} varies with the permittivity. Comparisons of dependence of two entries T_{0101} and T_{0501} are shown in Table 2 on permittivity and in Table 3 on aspect ratio, respectively.

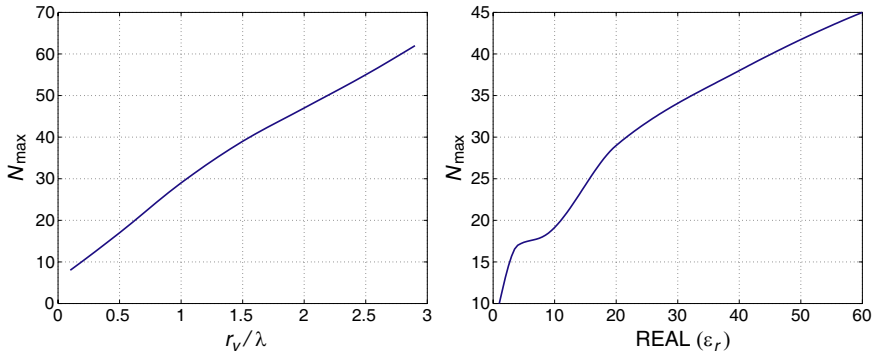

Figure 9. The size of T matrix $N_{\max}$ varies with r_v or $\mathrm{Re}(\epsilon_r)$.

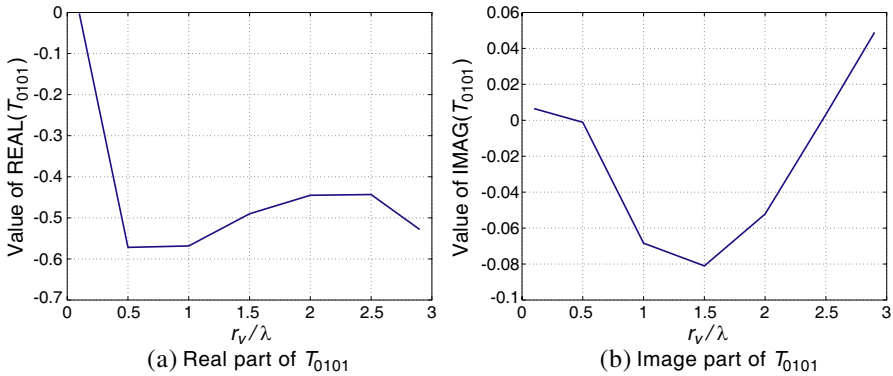

Figure 10. The value of term T_{0101} varies with r_v, where ρ is 1 and ϵ_r is $4 + i$.

Table 2. The values of term T_{0101} and T_{0501} versus ϵ_r for circular cylinder where ρ is 1 and r_v is 0.5.

ϵ_r	T_{0101}	T_{0501}
$1 + 0.25i$	$-0.26 - 1.38 \times 10^{-2}i$	$1.79 \times 10^{-3} - 2.25 \times 10^{-4}i$
$4 + i$	$-0.57 - 1.12 \times 10^{-3}i$	$2.43 \times 10^{-3} - 1.92 \times 10^{-2}i$
$8 + 2i$	$-0.74 + 7.06 \times 10^{-2}i$	$1.52 \times 10^{-2} - 1.39 \times 10^{-2}i$
$20 + 5i$	$-0.76 + 0.15i$	$2.00 \times 10^{-2} - 1.63 \times 10^{-2}i$
$40 + 10i$	$-0.80 + 0.17i$	$2.32 \times 10^{-2} - 1.46 \times 10^{-2}i$
$60 + 15i$	$-0.81 + 0.18i$	$2.46 \times 10^{-2} - 1.43 \times 10^{-2}i$

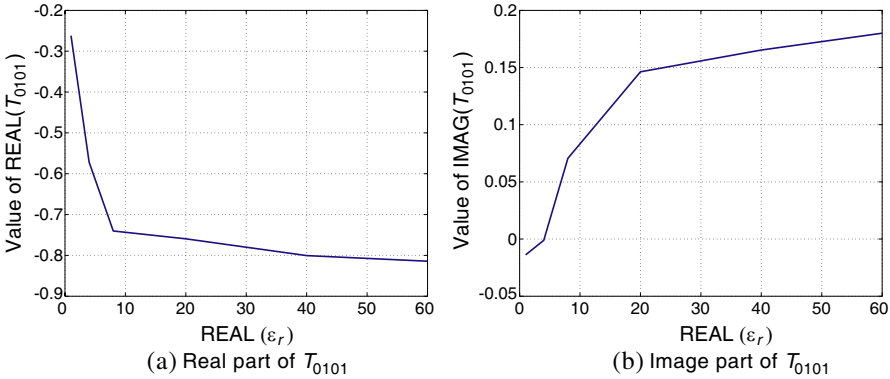

(a) Real part of T_{0101} (b) Image part of T_{0101}

Figure 11. The value of term T_{0101} varies with $\mathrm{Re}(\epsilon_r)$, where ρ is 1 and r_v is 0.5.

The numerical experiments for characterization of the convergence region against r_v and ϵ_r are carried out in a controlled manner so as to make the results more amenable to analysis. First the aspect ratio ρ is set to 1. The corresponding shape is closer to sphere than that of other values of ρ and hence possesses better convergence with the same other parameters. This choice is further warranted by the good convergence behavior of the proposed method for large aspect ratio. Next since the real and imaginary parts of the complex dielectric constant for a linear, temporally dispersive medium are related by the Kramers-Kronig relation [28], yet information of the susceptibility may not be readily available, we assume the real and imaginary parts of the complex dielectric constant change proportionally, an assumption that at least qualitatively depicts the trend and enables us to focus on the combinatory effect of the real part with the equivalent volumetric radius (r_v) in the convergence behavior.

Table 4 shows with changing complex dielectric constant, the values of the maximal size parameter represented by r_v that ensure convergency ($\Delta = 10^{-4}$), where the aspect ratio ρ is 1, and λ is the wavelength of the incidence wave. It is clear from the table that the maximal convergent size parameters strongly depend on the relative dielectric constant and tend to decrease as real part of the permittivity of the cylinder increases. The relation can be expressed in the following empirical formula

$$r_v = \lambda \left[6.85 \mathrm{Re}(\epsilon_r)^{-0.28} - 1.52 \right] \tag{17}$$

Table 3. The values of term T_{0101} and T_{0501} versus r_v for circular cylinder where ρ is 1 and ϵ_r is $4 + i$.

r_v	T_{0101}	T_{0501}
0.1	$-2.55 \times 10^{-3} + 6.51 \times 10^{-3} i$	$3.31 \times 10^{-8} - 8.72 \times 10^{-8} i$
0.5	$-0.57 - 1.12 \times 10^{-3} i$	$2.43 \times 10^{-3} - 1.92 \times 10^{-2} i$
1.0	$-0.57 - 6.84 \times 10^{-2} i$	$-4.85 \times 10^{-2} + 6.74 \times 10^{-2} i$
1.5	$-0.49 - 8.10 \times 10^{-2} i$	$-6.65 \times 10^{-2} - 3.16 \times 10^{-2} i$
2.0	$-0.45 - 5.22 \times 10^{-2} i$	$7.89 \times 10^{-3} - 5.46 \times 10^{-2} i$
2.5	$-0.44 + 3.30 \times 10^{-2} i$	$5.26 \times 10^{-2} - 2.56 \times 10^{-2} i$
2.9	$-0.53 + 4.88 \times 10^{-2} i$	$6.30 \times 10^{-3} + 5.14 \times 10^{-2} i$

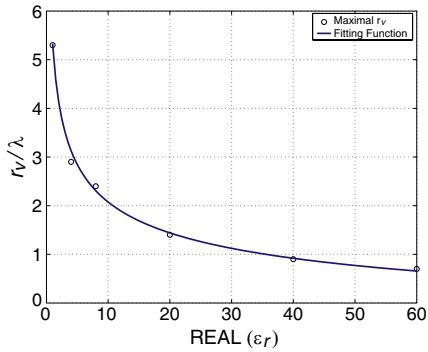

Figure 12. Plot of the maximal r_v versus relative dielectric constant ϵ_r for T matrix computation of a circular cylinder with aspect ratio $\rho = 1$.

Table 4. Maximal size parameter r_v versus relative dielectric constant ϵ_r for circular cylinder where the aspect ratio ρ is 1.

ϵ_r	$r_v(\lambda)$
$4+i$	2.9
$8+2i$	2.4
$20+5i$	1.4
$40+10i$	0.9
$60+15i$	0.7

For other complex dielectric constant where the susceptibility is different, the resultant relation between the real part of the permittivity and the maximal convergent size parameter is different from (17) yet the discrepancy is not expected to be significant. Hence the relation depicted in Fig. 12 is typical in upper bounding the combinatory effect of the real part with the equivalent volumetric radius (r_v) in the convergence behavior: any combination below the curve represents a convergent case while any above represents divergency.

6. CONCLUSION

Recently we proposed a method based on an extension of the T-matrix approach to analyze scattering from dielectric cylinders with finite length and large aspect ratio. In the current work we took advantage of a method of moment code we developed to fully characterize the region of validity of the proposed method. The proposed method is found to be applicable to dielectric cylinders of arbitrary length as long as the T matrix is attainable for the elementary sub-cylinder. The conditions for the T matrix to be numerically stably calculated in terms of the equivalent volumetric radius and relative dielectric constant are also empirically obtained. The proposed method is expected to be valuable in microwave remote sensing applications. The performances for finite cylinders with other cross section are currently under investigation.

ACKNOWLEDGMENT

This work was supported by National Basic Science Research and Development Grants (973) under Grant No. 2007CB714404, and

National High Technology "863" Programs of China under Grant No. 2009AA12Z113.

REFERENCES

1. Ulaby, F. T., K. Sarabandi, K. McDonald, M. Whitt, and M. C. Dobson, "Michigan microwave canopy scattering model," *Int. J. Remote Sensing*, Vol. 38, No. 7, 2097–2128, 2000.
2. Yueh, S. H., J. A. Kong, J. K. Jao, R. T. Shin, and T. L. Toan, "Branching model for vegetation," *IEEE Trans. Geosci. Remote Sensing*, Vol. 30, 390–402, 1992.
3. Chiu, T. and K. Sarabandi, "Electromagnetic scattering from short branching vegetation," *IEEE Trans. Geosci. Remote Sensing,* Vol. 38, No. 2, 911–925, 2000.
4. Du, Y., Y. Luo, W. Z. Yan, and J. A. Kong, "An electromagnetic scattering model for soybean canopy," *Progress In Electromagnetics Research*, PIER 79, 209–223, 2008.
5. Ahmed, S. and Q. A. Naqvi, "Electromagnetic scattering from parallel perfect electromagnetic conductor cylinders of circular cross-sections using an iterative procedure," *Journal of Electromagnetic Waves and Applications*, Vol. 22, No. 7, 987–1003, 2008.
6. Illahi, A., M. Afzaal, and Q. A. Naqvi, "Scattering of dipole field by a perfect electromagnetic conductor cylinder," *Progress In Electromagnetics Research Letters*, Vol. 4, 43–53, 2008.
7. Mishra, M. and N. Gupta, "Application of quasi Monte Carlo integration technique in EM scattering from finite cylinders," *Progress In Electromagnetics Research Letters*, Vol. 9, 109–118, 2009.
8. Valagiannopoulos, C. A., "Arbitrary currents on circular cylinder with inhomogeneous cladding and RCS optimization," *Journal of Electromagnetic Waves and Applications*, Vol. 21, No. 5, 665–680, 2007.
9. Karam, M. A. and A. K. Fung, "Electromagnetic wave scattering from some vegetation samples," *IEEE Trans. Geosci. Remote Sensing,* Vol. 26, 799–808, 1988.
10. Karam, M. A. and A. K. Fung, "Electromagnetic wave scattering from some vegetation samples," *Int. J. Remote Sensing,* Vol. 9, 1109–1134, 1988.
11. Waterman, P. C., "Matrix formulation of electromagnetic scattering," *Proc. IEEE,* Vol. 53, 805–811, 1956.

12. Mishchenko, M. I., L. D. Travis, and A. A. Lacis, *Scattering, Absorption, and Emission of Light by Small Particles,* Cambridge U. Press, 1985.
13. Mishchenko, M. I. and L. D. Travis, "T-matrix computations of light scattering by large spheroidal particles," *Opt. Commun.*, Vol. 109, 16–21, 1994.
14. Mishchenko, M. I., L. D. Travis, and A. Macke, "Scattering of light by polydisperse, randomly oriented, finite circular cylinders," *Appl. Opt.,* Vol. 35, 4927–4940, 1996.
15. Mishchenko, M. I., L. D. Travis, and D. W. Mackowski, "T-matrix computations of light scattering by nonspherical particles: A review," *J. Quant. Spectrosc. Radiat. Transfer,* Vol. 55, 535–575, 1996.
16. Wielaard, D. J., M. I. Mishchenko, A. Macke, and B. E. Carlson, "Improved T-matrix computations for large, nonabsorbing and weakly absorbing nonspherical particles and comparison with geometrical optics approximation," *Appl. Opt.,* Vol. 36, 4305–4313, 1997.
17. Mishchenko, M. I., "Calculation of the amplitude matrix for a nonspherical particle in a fixed orientation," *Appl. Opt.,* Vol. 39, 1026–1031, 2000.
18. Barber, P. W., "Resonance electromagnetic absorption by nonspherical dielectric objects," *IEEE Trans. Microwave Theory Tech.,* Vol. 25, 373–371, 1954.
19. Yan, W.-Z., Y. Du, H. Wu, D. Liu, and B.-I. Wu, "EM scattering from a long dielectric circular cylinder," *Progress In Electromagnetics Research,* PIER 85, 39–67, 2008.
20. Umashankar, K., A. Taflove, and S. M. Rao, "Electromagnetic scattering by arbitrary shaped three-dimensional homogeneous lossy dielectric objcts," *IEEE Trans. Antennas Propagat.*, Vol. 34, 758–766, 1986.
21. Rao, S. M., D. R. Wilton, and A. W. Glisson, "Electromagnetic scattering by surfaces of arbitrary shape," *IEEE Trans. Antennas Propagat.*, Vol. 30, 409–418, 1982.
22. Wang, L. F., J. A. Kong, K. H. Ding, T. Le Toan, F. Ribbes, and N. Floury, "Electromagnetic scattering model for rice canopy based on Monte Carlo simulation," *Progress In Electromagnetics Research,* PIER 52, 153–171, 2005.
23. Arslan, A. N., J. Pulliainen, and M. Hallikainen, "Observations of L-and C-band backscatter and a semi-empirical backscattering model approach from a forest-snow-ground system," *Progress In*

Electromagnetics Research, PIER 56, 263–281, 2006.

24. Stein, S., "Addition theorems for spherical ware functions," *Q. Appl. Math.,* Vol. 19, 15–24, 1961.
25. Tsang, L., J. A. Kong, and R. T. Shin, *Theory of Microwave Remote Sensing,* Wiley Interscience, New York, 1985.
26. Xu, Y. L., "Electromagnetic scattering by an aggregate of spheres," *Appl. Opt.,* Vol. 34, 4573–4588, 1995.
27. Mishchenko, M. I., "Light scattering by size-shape distributions of randomly oriented axially symmetric particles of size comparable to a wavelength," *Appl. Opt.,* Vol. 32, 4652–4666, 1993.
28. Kong, J. A., *Electromagnetic Wave Theory*, EMW Publishing, Cambridge, MA, 2005.